Testing Frequency-Domain Causality in Multivariate Time Series

Luca Faes*, *Member, IEEE*, Alberto Porta, *Member, IEEE*, and Giandomenico Nollo, *Member, IEEE*

***Abstract*—We introduce a new hypothesis-testing framework, based on surrogate data generation, to assess in the frequency domain, the concept of causality among multivariate (MV) time series. The approach extends the traditional Fourier transform (FT) method for generating surrogate data in a MV process and adapts it to the specific issue of causality. It generates causal FT (CFT) surrogates with FT modulus taken from the original series, and FT phase taken from a set of series with causal interactions set to zero over the direction of interest and preserved over all other directions. Two different zero-setting procedures, acting on the parameters of a MV autoregressive (MVAR) model fitted on the original series, were used to test the null hypotheses of absence of direct causal influence (CFTd surrogates) and of full (direct and indirect) causal influence (CFTf surrogates), respectively. CFTf and CFTd surrogates were utilized in combination with the directed coherence (DC) and the partial DC (PDC) spectral causality estimators, respectively. Simulations reproducing different causality patterns in linear MVAR processes demonstrated the better accuracy of CFTf and CFTd surrogates with respect to traditional FT surrogates. Application on real MV biological data measured from healthy humans, i.e., heart period, arterial pressure, and respiration variability, as well as multichannel EEG signals, showed that CFT surrogates disclose causal patterns in accordance with expected cardiorespiratory and neurophysiological mechanisms.**

***Index Terms*—Cardiovascular variability, directed coherence (DC), EEG, multivariate autoregressive (MVAR) models, partial directed coherence (PDC), surrogate data.**

I. Introduction

MULTIVARIATE (MV) time series analysis is extensively used to investigate the interactions among signals simultaneously recorded from physiological systems. Applications are ubiquitous, for instance, in neurophysiology [1] and cardiovascular physiology [2]. The analysis of interdependences in MV time series is traditionally performed at two stages: evaluation of the presence or absence of interactions, i.e., detection of coupling and evaluation of driver-response relationships, i.e., assessment of causality. While nonlinear approaches to coupling and causality detection are more general, linear methods have the important advantage to be strictly connected to the frequency-domain representation of multichannel data. In fact, evaluation of directional interactions within specific frequency bands is extremely useful for the study of physiological processes, which are rich in oscillatory content, and thus, lend themselves to spectral representation. While coupling is traditionally measured through the coherence function [3], several techniques based on linear MV autoregressive (MVAR) representation of multichannel data have been proposed to quantify causality in the frequency domain and applied to physiological time series [4]–[8]. Among them, the directed coherence (DC) [4], [5] and the partial DC (PDC) [7] functions are of great interest as they constitute factorizations of the ordinary coherence and of the partial coherence, respectively, able to elicit causality from the modeled interactions. While the PDC is a frequency-domain representation of the very popular concept of direct causality introduced by Granger [9], [10], the DC can detect both direct and indirect causal influences from one series to another in the spectral representation of MVAR processes [11].

An issue of great practical importance is the assessment of the significance of any frequency-domain index of coupling or causal coupling, such as the coherence, the DC, and the PDC. Due to practical estimation problems, nonzero values are indeed likely to occur at some frequencies even in the case of absence of a true interaction between the two considered series. This problem is commonly faced by means of a statistical hypothesis-testing approach based on setting a threshold for significance at the upper limit of the confidence interval of the considered index, where confidence intervals are based on the sampling (theoretical or empirical) distribution of the index computed under the null hypothesis of absence of interaction. Comparing at each specific frequency, the estimated index with the threshold allows rejection or acceptance of the null hypothesis according to the predetermined level of significance.

The theoretical distribution in absence of coupling has been derived for the coherence [12], PDC [13], and DC [11] estimators. However, as theoretical distributions are computed assuming large sample sizes, they may become unreliable in the presence of short data segments, typical of real applications. A viable, widely adopted alternative is to use the empirical distribution of the considered index for the estimation of a threshold for significance [5], [6], [8], [14]. The empirical distribution is commonly obtained computing the index over a set of surrogate time series, which are derived from the original series

Manuscript received October 29, 2009; revised December 30, 2009; accepted February 1, 2010. Date of publication February 18, 2010; date of current version July 14, 2010. This paper was presented in part at the 31st Annual International Engineering in Medicine and Biology Society (EMBC) Conference, Minneapolis, MN, September 2–6, 2009. *Asterisk indicates corresponding author.*

*L. Faes is with the Biophysics and Biosignals Laboratory, BioTech, University of Trento, 38060 Trento, Italy (e-mail: luca.faes@unitn.it).

A. Porta is with the Department of Technologies for Health, Galeazzi Orthopaedic Institute, University of Milan, 20161 Milan, Italy (e-mail: alberto.porta@unimi.it).

G. Nollo is with the Biophysics and Biosignals Laboratory, BioTech, University of Trento, 38060 Trento, Italy (e-mail: nollo@science.unitn.it).

Color versions of one or more of the figures in this paper are available online at http://ieeexplore.ieee.org.

Digital Object Identifier 10.1109/TBME.2010.2042715

by a procedure preserving their power spectra, but destroying their coupling. Among the many algorithms to generate surrogate data [15], Fourier transform (FT) surrogates [16], obtained by a phase randomization procedure applied independently to each series of the considered MV dataset, have been proposed to assess the significance of the coherence [14], and have been used also to test the significance of causal coupling measures in the frequency domain [5], [6], [8].

Unfortunately, the FT method produces surrogate time series, which are more uncoupled than required to test the hypothesis of nonzero causality. Indeed, the null hypothesis to which independent FT surrogates are consistent with, i.e., fully uncorrelated linear processes, imposes the disruption of causal interactions in any direction (i.e., even over directions different from the investigated one). Hence, the aim of this study is to introduce a novel approach, based on a modified FT algorithm, to generate surrogate data for the assessment of frequency-domain causality in MVAR processes. The main peculiarity of the approach is to destroy selectively causality only over the direction under study, while leaving untouched causal effects over pathways alternative to the considered one.

The paper is organized as follows. Section II introduces time- and frequency-domain approaches to assess causality in the context of MVAR processes. Section III introduces the new approach for surrogate data generation as an extension of the traditional FT approach and describes the statistical procedure utilized to test for frequency-domain causality. The new approach is validated on simulated MVAR processes in Section IV, while Section V is devoted to application of the method on real biomedical MV time series. Section VI concludes the paper. Part of this paper has been presented in a preliminary form at the 31st Annual International EMBC Conference [17].

II. Background

A. Causality and Coupling in MV Closed-Loop Processes

Consider M stationary stochastic processes y_m, $m = 1, \ldots, M$. Without loss of generality, we assume that the processes are defined at discrete time ($y_m = \{y_m(n)\}$, e.g., are sampled versions of the continuous-time processes $y_m(t)$, taken at the times $t_n = nT$, where T is the sampling period) and have zero mean. A MV closed-loop process is defined as follows:

$$y_m(n) = f_m\left(\bar{Y}_m, Y_k | k \neq m\right) + w_m(n),\ k,\ m = 1, \ldots, M \tag{1}$$

where f_m is the function linking the set of the p past values of the mth process $\bar{Y}_m = \{y_m(n-1), \ldots, y_m(n-p)\}$, as well as the sets of the present and the p past values of all other processes $Y_k = \{y_k(n), \bar{Y}_k\} = \{y_k(n), y_k(n-1), \ldots, y_k(n-p)\}$, $k \neq m$, to the present value $y_m(n)$, and w_m are uncorrelated white noise processes. Given two processes y_i and $y_l, i, l = 1, \ldots, M$, and denoting as $Z_{li} = \{\bar{Y}_l, Y_k,\ k = 1, \ldots M,\ k \neq i,\ k \neq l\}$ being the set of the past values of y_l, and the present and past values of all other processes except y_i, causality and coupling definitions are provided as follows. *Direct causality* from y_i to y_l, $y_i \rightarrow y_l$, exists if the prediction of $y_l(n)$ based on Z_{li} and Y_i is better than the prediction of $y_l(n)$ solely based on Z_{li}. *Causality* from y_i to y_l, $y_i \Rightarrow y_l$, exists if a cascade of L direct causality relations occurs, such that $y_{m_{s-1}}$ causes y_{m_s} for each $s = 1, \ldots, L (1 \leq m_s \leq M;\ m_s \neq i,\ m_s \neq l$ for $s < L;\ m_L = l,\ m_0 = i)$ for at least one $L \leq M - 1$. *Coupling* between y_i and y_l, $y_i \Leftrightarrow y_l$, exists if $y_i \Rightarrow y_l$ or $y_l \Rightarrow y_i$. According to these definitions, $y_i \rightarrow y_l$ implies $y_i \Rightarrow y_l$, but the reverse might not hold, while $y_i \Rightarrow y_l$ implies $y_i \Leftrightarrow y_l$, but the reverse might not hold. Indeed, causality is detected when direct or indirect causal relations are present and coupling is detected when forward or backward causal relations are present.

Note that for a bivariate closed-loop process ($M = 2$) causality reduces to direct causality. In this case, the definition agrees with the notion of Granger causality [9] involving only the relations between two processes. When $M \geq 3$ processes are considered, the definition of direct causality agrees with the definition of $primafacie$ cause given by Granger [10] and referred to as conditional Granger causality later on [18]. The definition of causality is an extension of direct causality including also indirect effects from one process to a second one, i.e., effects mediated by one or more other processes in the MV closed loop. Note also that the formulations of causality and direct causality here provided, can account for instantaneous interactions among processes, as some authors have suggested [19], [20], in addition to lagged interactions traditionally studied [9], [10].

B. Time-Domain Causality in MVAR Processes

Let us model an MV closed-loop process as a MVAR process

$$\mathbf{Y}(n) = \sum_{k=0}^{p} \mathbf{B}(k)\, \mathbf{Y}(n-k) + \mathbf{W}(n) \tag{2}$$

where $\mathbf{Y}(n) = [y_1(n), \ldots, y_M(n)]^{\mathrm{T}}$ and $\mathbf{W}(n) = [w_1(n), \ldots, w_M(n)]^{\mathrm{T}}$ are the column vectors of the observed processes, and of the white and uncorrelated input processes, respectively, and $\mathbf{B}(k)$ are $M \times M$ coefficient matrices in which the element $b_{li}(k)$ describes the direct causal dependence from y_i to y_l at lag $k (i, l = 1, \ldots, M; b_{ii}(0) = 0)$. Equation (2) is a particularization of (1) in which each function f_m is a linear first-order polynomial.

Given the representation in (2), the definitions of direct causality, causality, and coupling provided for a general closed-loop process can be specified for a MVAR process in terms of the off-diagonal elements of $\mathbf{B}(k)$ as follows: $y_i \rightarrow y_l$ if $b_{li}(k) \neq 0$ for at least one value of $k = 0, 1, \ldots, p$; $y_i \Rightarrow y_l$ if $b_{m_s m_{s-1}}(k_s) \neq 0$ for each $s = 1, \ldots, L\ (1 \leq m_s \leq M;\ m_s \neq i,\ m_s \neq l$ for $s < L;\ m_L = l,\ m_0 = i)$ for at least one $L \leq M - 1$ and one set of $k_1, \ldots, k_L = 0, 1, \ldots, p$; $y_i \Leftrightarrow y_l$ if $b_{m_s m_{s-1}}(k_s) \neq 0$ for each $s = 1, \ldots, L$ with $(m_0 = i, m_L = l)$ or with $(m_0 = l, m_L = i)$ for at least one L and at least one set of $k_1, \ldots, k_L$. Thus, direct causality, causality, and coupling are found when the direct path from y_i to y_l, when at least one (direct or indirect) path from y_i to y_l, and when at least one (forward or backward) path between y_i and y_l, is significant, respectively (i.e., described by nonzero coefficients in $\mathbf{B}$).

C. Frequency-Domain Causality in MVAR Processes

The spectral representation of the MVAR process (2) is obtained by applying the FT operator: $\Im\{\mathbf{Y}(n)\} = \mathbf{Y}(f) = \Sigma_{n=-\infty}^{\infty} \mathbf{Y}(n)\, e^{-i2\pi f n T}$, yielding $\bar{\mathbf{B}}(f)\,\mathbf{Y}(f) = \mathbf{W}(f)$, where $\bar{\mathbf{B}}(f) = \mathbf{I} - \Sigma_{k=0}^{p} \mathbf{B}(k)\, e^{-i2\pi f k T}$ is the coefficient matrix in the frequency domain ($\mathbf{I}$ is the $M \times M$ identity matrix). To evidence the transfer function matrix from $\mathbf{W}(n)$ to $\mathbf{Y}(n)$, the spectral representation is rewritten as $\mathbf{Y}(f) = \mathbf{H}(f)\,\mathbf{W}(f)$, where $\mathbf{H}(f) = \bar{\mathbf{B}}^{-1}(f)$ is the $M \times M$ transfer matrix in the frequency domain. Given the assumption of whiteness and uncorrelation of the input processes, the spectral power density matrix of $\mathbf{Y}(n)$ can be factored as $\mathbf{S}(f) = \mathbf{H}(f)\,\mathbf{\Sigma_W}\,\mathbf{H}^{\mathrm{H}}(f)$, where the superscript H stands for Hermitian transpose and $\mathbf{\Sigma_W} = \mathrm{diag}\left(\sigma_i^2\right)$ is the diagonal covariance matrix of $\mathbf{W}(n)$.

The elements of the spectral density, transfer function, and coefficient matrices can be used to measure coupling and causality in the frequency domain. Specifically, the coherence [3], the DC [4], and the PDC [7], [21] are defined, respectively, as follows:

$$C_{li}(f) = \frac{S_{li}(f)}{\sqrt{S_{ii}(f)\,S_{ll}(f)}}, \qquad \gamma_{li}(f) = \frac{\sigma_i H_{li}(f)}{\sqrt{S_{ll}(f)}},$$
$$\pi_{li}(f) = \frac{\frac{1}{\sigma_l}\bar{B}_{li}(f)}{\sqrt{\sum_{m=1}^{M} \frac{1}{\sigma_m^2} |\bar{B}_{mi}(f)|^2}} \tag{3}$$

where $S_{li}(f)$, $H_{li}(f)$, and $\bar{B}_{li}(f)$ are the *l*,*i* elements of $\mathbf{S}(f)$, $\mathbf{H}(f)$, and $\bar{\mathbf{B}}(f)$. To have real values related to the magnitude of the aforementioned functions, the squared absolute values of (3) are commonly computed as measures of coupling strength. Specifically, the squared coherence $C_{li}^2(f) = C_{il}^2(f)$ quantifies the strength of the noncausal coupling between the processes y_i and y_l at the frequency f. The squared DC $\gamma_{li}^2(f)$ quantifies the strength of the causal coupling from y_i to y_l as normalized contribution of y_i to the power spectrum of y_l at the frequency f. Such a contribution is related to both direct and indirect causal links, since expanding $\mathbf{H}(f) = \bar{\mathbf{B}}^{-1}(f)$ as a geometric series, one can show that $H_{li}(f)$ contains a sum of terms each one related to one of the (direct or indirect) transfer paths connecting y_i to y_l [11]. The squared PDC $\pi_{li}^2(f)$ quantifies the strength of the causal coupling from y_i to y_l as a quantity related to the magnitude of the link from y_i to y_l at the frequency f normalized by the effects related to the presence of the other processes y_m, $m \neq i, m \neq l$; in (3) we use the generalized PDC definition [21] introducing a normalization useful in the presence of unbalanced w_i variances. Note that the PDC measures only direct causal contributions as it is defined from $\bar{B}_{li}(f)$, which contains a combination of $b_{li}(k)$.

Based on the aforementioned considerations, we observe that coherence, DC, and PDC can be regarded as frequency domain measures of coupling, causal coupling, and direct causal coupling between two processes. Thus, frequency-domain extensions of the time-domain definitions given in Section II-B are intuitively provided as follows: direct causality ($y_i \rightarrow y_l$), causality ($y_i \Rightarrow y_l$), and coupling ($y_i \Leftrightarrow y_l$) at the frequency f exist if $\pi_{li}^2(f) > 0$, $\gamma_{li}^2(f) > 0$, and $C_{li}^2(f) > 0$, respectively.

III. Methods

A. FT Surrogates

Let us consider the $M \times N$ MV series $\mathbf{Y}(n) = [y_1(n), \ldots, y_M(n)]^{\mathrm{T}}$, $n = 0, \ldots, N$–1, be a finite-length realization of the vector stochastic process defined earlier (*N* is the series length). For each series $y_m(n)$, an FT surrogate series $\bar{y}_m(n)$, was obtained by: 1) applying the discrete FT operator: $Y_m(f) = \Im\{y_m(n)\} = A_m(f)e^{i\varphi_m(f)}$, where the complex valued $Y_m(f)$ was evaluated at the discrete frequencies $f = k/(NT)$, $k = 0, \ldots, N-1$; 2) substituting the Fourier phase $\varphi_m(f)$ with a realization of a random variable $\theta_m(f)$ uniformly distributed in the range [0, 2π) while keeping constant the Fourier amplitude $A_m(f)$; and 3) taking the inverse FT: $\bar{y}_m(n) = \Im^{-1}\{A_m(f)e^{i\theta_m(f)}\}$ [16]. The surrogate series $\bar{y}_m(n)$, $m = 1, \ldots, M$, preserve the power spectrum of the original series $y_m(n)$, but provided that the random phases $\theta_m(f)$ are independent, are fully uncoupled to each other. These surrogates will be referred to as FT surrogates in the following sections.

B. Causal FT Surrogates

We propose a method for generating surrogate data, denoted as causal FT (CFT) surrogates in which the causal coupling is destroyed only over some directions of interactions, and is preserved over the remaining directions. This task was achieved first by fitting the MV time series with a MVAR model as in (2). After identification (see Appendix), we forced to zero some of the model coefficients depending on the type of frequency-domain causality from y_i to y_l, we wanted to investigate: 1) to test for causality $y_i \Rightarrow y_l$, we set to zero all the coefficients describing the direct dependencies originating from y_i: $b_{mi}(k) = 0$, $m = 1, \ldots, M(m \neq i), k = 0, 1, \ldots, p$, as well as the direct dependencies ending into y_l: $b_{lm}(k) = 0$, $m = 1, \ldots, M(m \neq l)$, $k = 0, 1, \ldots, p$; 2) to test for direct causality $y_i \rightarrow y_l$, we set to zero all coefficients describing the direct dependence from y_i to y_l : $b_{li}(k) = 0$, $k = 0, 1, \ldots, p$. After zeroing of the appropriate coefficients, the reduced model was iterated using *M* independent white noise realizations as input $\mathbf{W}(n)$ in (2) to get the series $\hat{\mathbf{Y}}(n) = [\hat{y}_1(n), \ldots, \hat{y}_M(n)]^{\mathrm{T}}$. The CFT surrogates were generated by: applying the discrete FT operator to the original series: $Y_m(f) = \Im\{y_m(n)\} = A_m(f)e^{i\varphi_m(f)}$, as well as to the series derived from simulating the reduced model: $\hat{Y}_m(f) = \Im\{\hat{y}_m(n)\} = \hat{A}_m(f)\, e^{i\hat{\varphi}_m(f)}$; imposing the Fourier amplitudes of the original series and the Fourier phases of the fitted series, respectively, as amplitudes and phase angles of the frequency-domain representation of the surrogates: $\tilde{Y}_m(f) = A_m(f)e^{i\hat{\varphi}_m(f)}$, and finally, returning to the time domain: $\tilde{y}_m(n) = \Im^{-1}\{\tilde{Y}_m(f)\}$. The CFT surrogates $\tilde{y}_m(n)$, $m = 1, \ldots, M$, preserved the power spectrum of the original series $y_m(n)$, as well as the phase differences among time series in accordance with the model (2), where causality from y_i to y_l was switched off. Surrogates obtained using the zero-setting procedures 1) and 2) were denoted as CFTf and CFTd surrogates, to indicate that they destroy the full (direct and indirect)

causal coupling, or only the direct causal coupling, respectively, along the considered direction of interaction.

C. Testing for Coupling and Causality in Frequency Domain

The significance of direct causality, causality, and coupling between two of the *M* observed time series was investigated in the frequency domain by the statistical approach known as the method of surrogate data [16]. This approach is based on: 1) a null hypothesis against which observations are tested; 2) a set of surrogate time series, which according to the null hypothesis, share the properties of the original series, but lack of the investigated property; 3) a discriminating statistic, which is sensitive to the investigated property; and 4) a statistical test performing a comparison of the values of the discriminating statistic computed for original and surrogate series.

Three null hypotheses were specified according to the definitions of coupling, causality, and direct causality provided earlier, i.e., the observed series are a realization of a MVAR process with absence of coupling between y_i and $y_l(h_1)$, absence of causality from y_i to $y_l(h_2)$, or absence of direct causality from y_i to $y_l(h_3)$. For surrogate series generation, we considered the three procedures described in Secttions III-A and III-B. Since CFTf and CFTd surrogates do not destroy the coupling between y_i and y_l, they are not consistent with h_1. Moreover, CFTd surrogates destroy only the direct causal coupling from y_i to y_l, but not the indirect, thus they are not consistent with h_2. On the contrary, FT surrogates are consistent with all the three hypotheses as they destroy any type of coupling (direct and indirect that occurs along forward and backward directions). Hence, FT, CFTf, and CFTd surrogates were used to test for $\{h_1, h_2, h_3\}$, for $\{h_2, h_3\}$, and for h_3, respectively. The discriminating statistics used to test the null hypotheses h_1, h_2, and h_3 were the squared coherence $C^2_{li}(f)$, the squared DC $\gamma^2_{li}(f)$, and the squared PDC $\pi^2_{li}(f)$, respectively, computed as in (3) after estimation of the MVAR coefficients as outlined in the Appendix. As statistical test, we performed a nonparametric test based on percentiles with 5% significance. The test compared, at each frequency f, the discriminating statistic computed over the original MV series with a threshold for significance set at the 95th percentile of the empirical distribution of the statistic computed over 500 sets of surrogate MV series. If the original value of the discriminating statistic was higher than the threshold, the null hypothesis was rejected and the investigated property (i.e., coupling, causality, or direct causality) was detected at the frequency *f*. If, on the contrary, the value was below the threshold, the original series were interpreted as consistent with the considered null hypothesis.

IV. Method Validation

A. Simulation Design

In the first simulation, we considered short realizations ($N = 300$ points, $T = 1$) of the linear MVAR process ($M = 3$)

$$y_1(n) = 2\rho\cos(2\pi f_1)\, y_1(n-1) - \rho^2 y_1(n-2) + w_1(n)$$
$$y_2(n) = 2\rho\cos(2\pi f_2)\, y_2(n-1) - \rho^2 y_2(n-2) + y_1(n-1) + w_2(n)$$
$$y_3(n) = 0.5 y_2(n-1) + w_3(n)$$

with $\rho = 0.97$, $f_1 = 0.1$, and $f_2 = 0.3$, where $w_i(n)$, $i = 1, 2, 3$, were realizations of uncorrelated white Gaussian noise processes with zero mean and unit variance [WGN(0,1)]. The series y_1 and y_2 exhibit autonomous narrowband oscillations at 0.1 and 0.2 Hz due to the diagonal values of the coefficient matrix $(b_{ii}(1) = 2\,\rho\cos 2\pi f_i,\ b_{ii}(2) = -\rho^2;\ i = 1, 2)$ generating complex-conjugate poles with modulus ρ and phases $2\pi f_1$ and $2\pi f_2$. Causal interactions were determined by the nonzero off-diagonal values of the coefficient matrix, i.e., $b_{21}(1) = 1$ and $b_{32}(1) = 0.5$. Thus, the imposed frequency-domain direct causality relations were $y_1 \rightarrow y_2$ at f_1 and $y_2 \rightarrow y_3$ at f_2, which determined causality relations $y_1 \Rightarrow y_2$ at f_1, $y_2 \Rightarrow y_3$ at f_2 and $y_1 \Rightarrow y_3$ at f_1, and coupling relations $y_1 \Leftrightarrow y_2$ at f_1, $y_2 \Leftrightarrow y_3$ at f_2 and $y_1 \Leftrightarrow y_3$ at f_1.

In the second simulation, we considered the linear MVAR process ($M = 4$, $N = 300$, $T = 1$)

$$y_1(n) = 2\rho_1\cos(2\pi f_1)\, y_1(n-1) - \rho_1^2 y_1(n-2) + w_1(n)$$
$$y_2(n) = 2\rho_2\cos(2\pi f_2)\, y_2(n-1) - \rho_2^2 y_2(n-2) + 0.4 y_1(n) - 0.3 y_3(n-1) + w_2(n)$$
$$y_3(n) = 2\rho_3\cos(2\pi f_3)\, y_3(n-1) - \rho_3^2 y_3(n-2) + 0.3 \times y_2(n-1) + 0.4 y_2(n-2) + w_3(n)$$
$$y_4(n) = 0.8 y_1(n-1) + 0.4 y_2(n-2) + w_4(n)$$

with $\rho_1 = \rho_2 = 0.9$, $\rho_3 = 0.95$, $f_1 = 0.1$, $f_2 = 0.2$, and $f_3 = 0.3$, where $w_1(n)$ and $w_3(n)$ were WGN(0,1), and $w_2(n)$ and $w_4(n)$ were WGN(0,2). The series y_1, y_2 and y_3 exhibit autonomous oscillations at 0.1, 0.2, and 0.3 Hz. The imposed direct causal effects, determined by $b_{li}(k)$ with $l \neq i$, were $y_1 \rightarrow y_2$ and $y_1 \rightarrow y_4$ at f_1, $y_2 \rightarrow y_3$ and $y_2 \rightarrow y_4$ at f_2, and $y_3 \rightarrow y_2$ at f_3, determining equivalent causality and coupling relations. Moreover, the presence of indirect effects $y_1 \rightarrow y_2 \rightarrow y_3$ and $y_3 \rightarrow y_2 \rightarrow y_4$ determined the causality and coupling relations $y_1 \Rightarrow y_3$, $y_1 \Leftrightarrow y_3$ at f_1, and $y_3 \Rightarrow y_4$, $y_3 \Leftrightarrow y_4$ at f_3.

B. Simulation Results

Figs. 1 and 2 report examples of the analysis performed for a single realization of the two simulations. The presence of coupling, causality, and direct causality was tested with the coherence using FT surrogates, with the DC using FT and CFTf surrogates, and with the PDC using FT, CFTf, and CFTd surrogates, respectively. The comparison between each spectral function and the corresponding thresholds was performed at the frequency of the imposed coupling, causality, or direct causality interaction.

In the first simulation, the expected coupling relations were detected by the coherence values $C^2_{12}(f_1)$, $C^2_{13}(f_1)$, and $C^2_{23}(f_2)$, exceeding the FT surrogate threshold [see Fig. 1(a)]. A significant coupling between y_2 and y_3 was

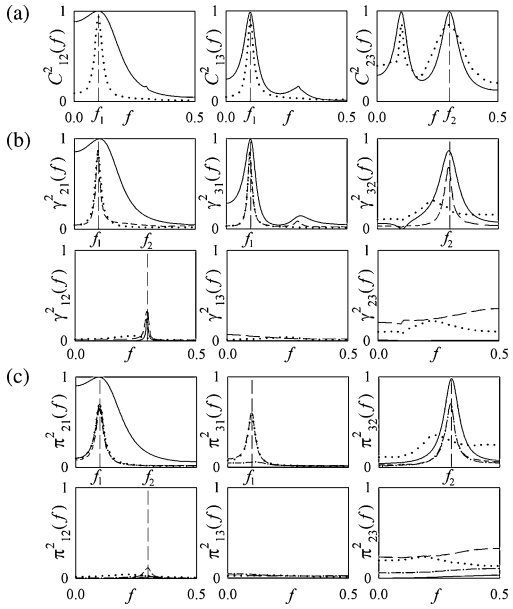

Fig. 1. Frequency-domain analysis for a realization of the first simulation. (a) Squared coherence between y_i and y_l ($C^2_{li}(f)$). (b) Squared DC from y_i to y_l ($\gamma^2_{li}(f)$). (c) Squared PDC from y_i to y_l ($\pi^2_{li}(f)$). Coherence, DC, and PDC (solid lines) are plotted together with their corresponding threshold for significance estimated using FT surrogates (dotted lines), CFTf surrogates (dashed lines), CFTd surrogates (dashed–dotted lines). Vertical lines mark the expected frequency (f_1 or f_2) of interaction for the considered series pair.

observed also at f_1, due to the common effect of y_1 over y_2 and y_3. The causality relations $y_1 \Rightarrow y_2$, $y_1 \Rightarrow y_3$, and $y_2 \Rightarrow y_3$, were correctly detected both by FT and CFTf surrogate procedures, as $\gamma^2_{21}(f_1)$, $\gamma^2_{31}(f_1)$, and $\gamma^2_{32}(f_2)$ are higher than the significance thresholds [see Fig. 1(b)]. Absence of causality was also noticed by both approaches over the directions $y_3 \Rightarrow y_1$ and $y_3 \Rightarrow y_2$, while the absence of causality $y_2 \Rightarrow y_1$ at f_2 was detected only by CFTf surrogates, but not by FT surrogates as $\gamma^2_{12}(f_2)$ exceeded the FT threshold giving an erroneous indication of causality. As regards detection of direct causality [see Fig. 1(c)], all surrogate procedures provided correct interpretation, since only the direct relations $y_1 \rightarrow y_2$ at f_1 and $y_2 \rightarrow y_3$ at f_2 were detected by the significant PDCs π^2_{21} and π^2_{32}, while all other relations were discarded.

In the second simulation, all the expected coupling relations were detected by the significant values of the coherence sampled at the frequencies of interest [dashed lines in Fig. 2(a)], due to the common influence of a third variable over the two considered variables, the coupling is deemed as significant for some other frequencies [e.g., $C^2_{23}(f_1)$ and $C^2_{24}(f_1)$]. The detection of causality was depicted by the significant squared DCs $\gamma^2_{21}(f_1)$, $\gamma^2_{31}(f_1)$, $\gamma^2_{41}(f_1)$, $\gamma^2_{32}(f_2)$, $\gamma^2_{42}(f_2)$, $\gamma^2_{43}(f_3)$, and $\gamma^2_{23}(f_3)$ according to both FT and CFTf surrogates [see Fig. 2(b)]. The hypothesis h_2 of absence of causality was accepted over the remaining directions, except from y_3 to y_1, where the DC $\gamma^2_{13}(f_3)$ seems slightly above the FT surrogate threshold. Regarding direct causality [see Fig. 2(c)], a correct interpretation was given by the combined use of PDC and CFTd surrogates, indeed, the hypothesis h_3 of absence of direct causality was accepted over the directions $y_1 \rightarrow y_2, y_1 \rightarrow y_4, y_2 \rightarrow y_3, y_2 \rightarrow y_4$, and $y_3 \rightarrow y_2$, and rejected over all other directions. Utilization of FT or CFTf surrogates led to misdetection of the direct causal couplings $y_1 \rightarrow y_2$ and $y_2 \rightarrow y_4$, as seen by the values of $\pi^2_{21}(f_1)$ and $\pi^2_{42}(f_2)$ not exceeding the zero-level thresholds.

The robustness of the earlier results was verified over 100 realizations of the simulations. For both simulations, all the expected coupling relations were always significant as the estimated coherence exceeded the FT surrogate threshold in all realizations. Thus, the results reported in Figs. 3 and 4 are limited to the analysis of causality and direct causality. Causality relations were assessed comparing the estimated DC with the threshold resulting from FT and CFTf surrogates. The results suggest that CFTf surrogates have similar sensitivity to FT surrogates, but may have higher specificity, e.g., the percentage of false positives was significantly higher, according to the McNemar test on paired proportions for FT than for CFTf surrogates, considering $\gamma^2_{12}(f_2)$ in the first simulation (see Fig. 3) and $\gamma^2_{13}(f_3)$ in the second simulation (see Fig. 4). False positives are likely due to the presence in the signals of multiple narrowband oscillations that cannot be assigned by FT surrogates to the correct source, as phase randomization destroys the full coupling within the MVAR process.

As direct causality may be tested using either FT, CFTf, or CFTd surrogates, we compared the performance of the three approaches in detecting the significance of the PDC using the Cochran *Q*-test for MV paired proportions. Results were comparable for the first simulation (see Fig. 3), while the second simulation (see Fig. 4) indicated that CFTd surrogates have the same specificity, but may have higher sensitivity than FT and CFTf surrogates, e.g., the percentage of true positives detections of direct causality was significantly higher for the PDCs $\pi^2_{21}(f_1)$, $\pi^2_{32}(f_2)$, and $\pi^2_{42}(f_2)$.

V. Application on Biomedical Time Series

This section describes the application of the proposed method on real MV biological time series. In all applications, the McNemar test for paired proportions was used to assess the statistical significance of the difference between the number of subjects showing significant causal coupling over the two directions of each considered pairwise interaction.

A. Cardiovascular Variability Analysis

Short-term cardiovascular and cardiorespiratory interactions were studied in eight young healthy subjects (22–27 years old) undergoing noninvasive recordings (1 kHz sampling rate) of surface ECG, finger photopletismographic arterial blood pressure (Finapres), and respiratory nasal flow (by differential pressure transducer) while lying in the supine position and spontaneously breathing. The beat-to-beat time series of heart period (RR interval), systolic arterial pressure (SAP), and respiratory flow (RF) were offline measured as the sequences of the temporal distances between consecutive R waves of the ECG, the local maxima of the arterial pressure signal inside each detected RR interval, and the values of the respiratory signal sampled at the onset of each RR interval, respectively. In each subject,

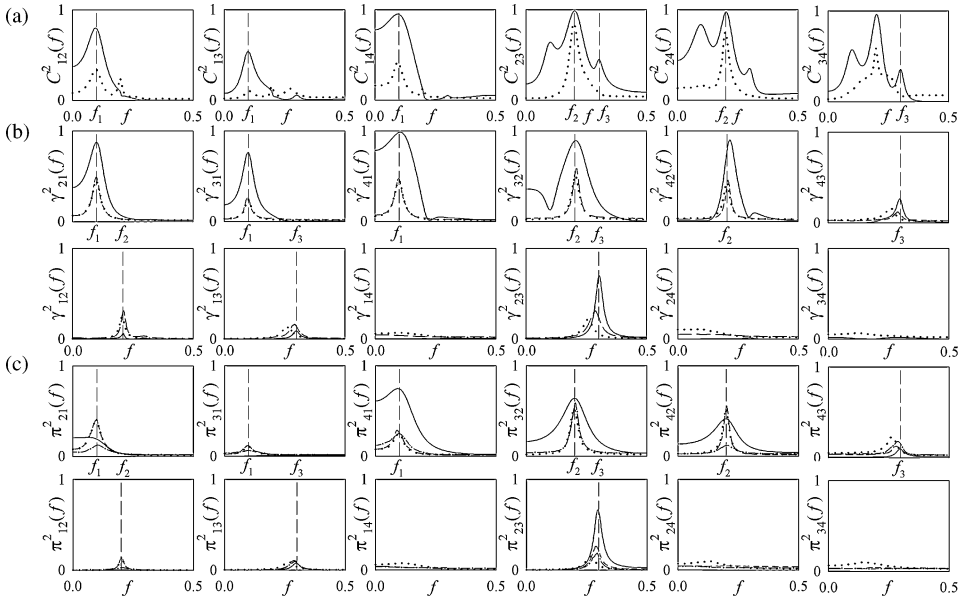

Fig. 2. Frequency-domain analysis for a realization of the second simulation. Plots and symbols are as in Fig. 1.

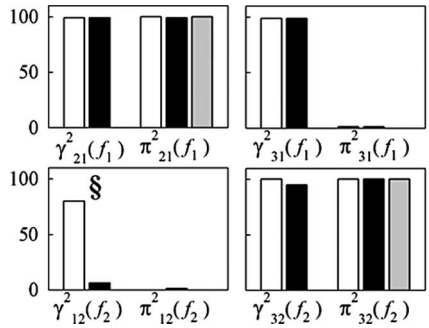

Fig. 3. Summary of frequency-domain causality tests for the first simulation. Bars are the percentage of realizations for which the squared DC γ^2_{li} and the squared PDC π^2_{li}, sampled at the frequency of the driving series, was larger than the threshold for significance derived from FT surrogates (white), CFTf surrogates (black), or CFTd surrogates (gray). §, $p < 0.001$ McNemar test CFTf versus FT for DC evaluation; #, $p < 0.001$ Cochran Q test CFTd versus FT and CFTd versus CFTf for PDC evaluation.

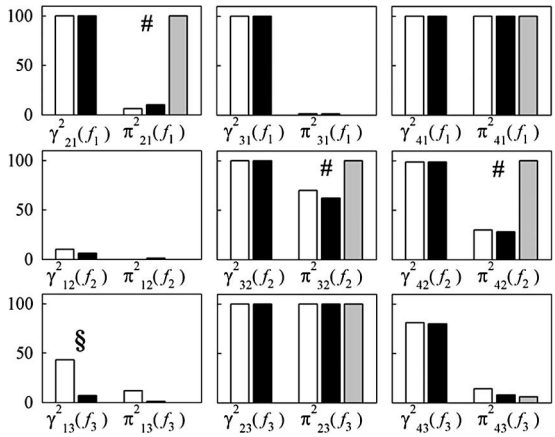

Fig. 4. Summary of frequency-domain causality tests for the second simulation. Symbols are as in Fig. 3.

synchronous stationary windows of RF (y_1), SAP (y_2), and RR (y_3) were selected for the analysis ($M = 3$ series, $N = 300$ samples, sampling period $T =$ mean RR).

In a representative subject, power spectrum analysis [see Fig. 5(a)] evidences the presence of a prominent spectral peak at the respiratory frequency for the RF series (S_{11}), while the power spectra of SAP (S_{22}) and RR (S_{33}) display the typical peaks in the LF (0.04–0.15 Hz) and HF ($\pm$0.04 Hz around the respiratory rate) bands [24]. The coherence analysis [see Fig. 5(b)] shows significant coupling relations between SAP and RR at LF, and between each pair of variables at HF. The analysis of the DC [see Fig. 5(c)] shows evident unidirectional causality relations RF $\Rightarrow$ SAP and RF $\Rightarrow$ RR at the frequency of respiration ($\gamma^2_{21}(\mathrm{HF})$ and $\gamma^2_{31}(\mathrm{HF})$ are significant, while $\gamma^2_{12}(\mathrm{HF})$ and $\gamma^2_{13}(\mathrm{HF})$ are nonsignificant). At LF, CFTf surrogates suggest unidirectional causality RR $\Rightarrow$ SAP (only $\gamma^2_{23}(\mathrm{LF})$ is significant), while FT surrogates suggest a mutual interaction (both $\gamma^2_{32}(\mathrm{LF})$ and $\gamma^2_{23}(\mathrm{LF})$ are significant); note that FT surrogates deem as significant also the small LF peak of γ^2_{13}. The analysis of direct causality [see Fig. 5(d)] helps to elucidate direct connections, e.g., showing that effects of RF are direct on RR (RF $\rightarrow$ RR as $\pi^2_{31}(\mathrm{HF})$ is significant) and both direct and indirect on SAP (RF $\rightarrow$ SAP as $\pi^2_{21}(\mathrm{HF})$ is significant, but also RF $\rightarrow$ RR $\rightarrow$ SAP as $\pi^2_{31}(\mathrm{HF})$ and $\pi^2_{23}(\mathrm{HF})$ are significant). Note that $\pi^2_{32}(\mathrm{LF})$ resulted nonsignificant only using CFTd surrogates.

Results extended to the eight subjects are summarized in Table I. The expected presence of interactions between RR interval and SAP in the LF band, and between all variables in the HF band [24], was documented in all subjects by the significant values of the coherence. At LF, a prevalence of the direct mechanical causal effects of RR on SAP [8] over the direct neural effects of SAP on RR [23] was documented by the higher DC and PDC values [$\gamma^2_{23}(\mathrm{LF}) > \gamma^2_{32}(\mathrm{LF})$, $\pi^2_{23}(\mathrm{LF}) > \pi^2_{32}(\mathrm{LF})$]. This unbalanced RR–SAP regulation at LF is in agreement with

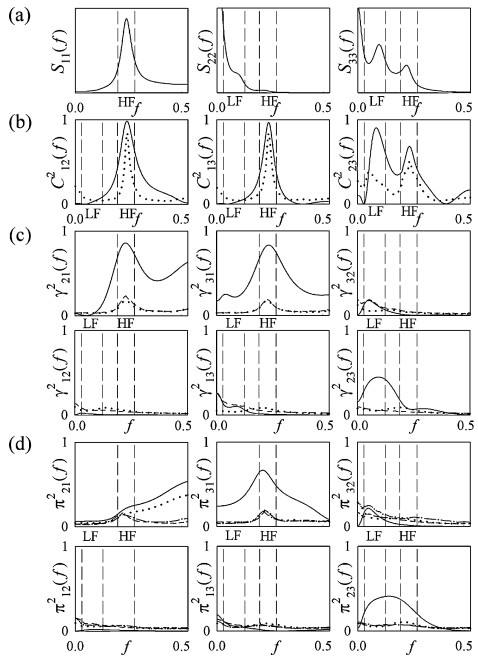

Fig. 5. Frequency-domain analysis of the RF (y_1), systolic pressure (y_2), and RR interval (y_3) time series in a representative subject. (a) Power spectral density of y_i ($S_{ii}(f)$). (b) Squared coherence between y_i and y_l ($C^2_{li}(f)$). (c) Squared DC from y_i to y_l ($\gamma^2_{li}(f)$). (d) Squared PDC from y_i to y_l ($\pi^2_{li}(f)$). Coherence, DC, and PDC (solid lines) are plotted together with their corresponding threshold for significance estimated using FT surrogates (dotted lines), CFTf surrogates (dashed lines), CFTd surrogates (dashed–dotted lines). Vertical lines mark the boundaries of LF and HF bands.

TABLE I
SUMMARY OF FREQUENCY-DOMAIN ANALYSIS FOR RF (y_1), SAP (y_2), AND RR INTERVAL (y_3) TIME SERIES

	C	n_{FT}	DC	n_{FT}	n_{CFTf}	PDC	n_{FT}	n_{CFTf}	n_{CFTd}
LF band									
1→2	0.07	0	-	-	-	-	-	-	-
2→1			0.01	0	0	0.01	0	0	0
1→3	0.09	0	-	-	-	-	-	-	-
3→1			0.05	0	3	0.03	0	0	0
2→3	0.49	8	0.12	3	6	0.13	3	5	5
3→2			0.38	8§	8	0.39	8§	8	8
HF band									
1→2	0.79	8	0.72	8	8	0.41	7	4	4
2→1			0.02	0§	0§	0.02	0§	0§	0§
1→3	0.69	8	0.62	8	8	0.37	8	6	6
3→1			0.03	0§	0§	0.02	0§	0§	0§
2→3	0.70	8	0.02	0	0	0.01	0	0	0
3→2			0.11	4§	4§	0.24	6§	6§	6§

At each connection $i\to l$, noninteger values are the mean over subjects of the coherence (C) between y_i and y_l, the DC from y_i to y_l, and the PDC from y_i to y_l, measured as average value within the LF and HF bands; integer values (n_{FT}, n_{CFTf}, n_{CFTd}) are the number of subjects showing significant coupling inside the considered frequency band according to FT, CFTf, and CFTd surrogate procedures. DC and PDC with y_1 as input signal are not calculated at LF due to the absence of LF oscillations of the RF. §, $p < 0.05$ McNemar test between values of n over the two directions of a pairwise interaction.

the notion that the mechanical feedforward pathway (from RR to SAP) plays a greater role than the baroreflex feedback pathway (from SAP to RR) in the LF cardiovascular regulation in supine humans [8]. In terms of number of subjects showing significant causal coupling, the unbalance was statistically significant only using the appropriate surrogates, i.e., CFTf surrogates with the DC and CFTd surrogates for the PDC. Note also that utilization of FT surrogates to assess causality led to a physiologically unlikely result, i.e., the presence of a significant DC from RR to RF γ^2_{13}(LF), in three out of eight subjects. At HF, both the DC values and the number of subjects showing significant causality according to FT and CFTf surrogates evidenced the unidirectional coupling from respiration to SAP and to RR. Moreover, utilization of the PDC together with CFTd surrogates put emphasis on different physiological mechanisms. The significance of the PDC from RF to RR π^2_{31}(HF) should reflect the well-known respiratory sinus arrhythmia phenomenon [24]. Indirect effects RF → SAP → RR mediated through the baroreflex are not highlighted here, since the PDC from SAP to RR π^2_{32}(HF), was never significant. On the contrary, the unidirectional interaction from RF to SAP seems to occur both along the direct pathway RF → SAP [see the significance of π^2_{21}(HF)], reflecting the mechanical effects of respiration on the arterial pressure variability [25], and along the indirect pathway RF → RR → SAP [see the significance of π^2_{31}(HF) and π^2_{23}(HF)], reflecting the projection of respiratory sinus arrhythmia effects on the vasculature, probably through mechanical coupling [8].

B. EEG Analysis

Multichannel ($M = 4$) EEG were recorded (10–20 system, 256 Hz sampling rate, common reference at electrode Fpz) in eight healthy young subjects (24–29 years old) resting with eyes closed in the relaxed awake state. Signals were bandpass filtered (FFT filter, 0.3–40 Hz), and then, downsampled to 64 Hz. Four bipolar signals taken as representative of different cortical areas were then obtained in each subject differentiating pairs of adjacent common-referenced signals ($y_1 = \mathrm{O1} - \mathrm{O2}$: occipital area, $y_2 = \mathrm{T3} - \mathrm{C3}$: left central area, $y_3 = \mathrm{C4} - \mathrm{T4}$: right central area, and $y_5 = \mathrm{Fp1} - \mathrm{Fp2}$: frontal area). Artefact free, stationary windows of 5 s duration ($N = 320$ samples, sampling period $T = 15.6$ ms) were then selected for the analysis.

In a representative subject, the power spectral density [see Fig. 6(a)] displays for all series a peak in the α-frequency band (8–13 Hz). The coherence [see Fig. 6(b)] suggest a significant coupling between each pair of signals, except for the coupling $y_3 \Leftrightarrow y_4$, within the α-band. The frequency-domain connectivity pattern depicted by the DC [see Fig. 6(c)] evidences a prevalent back-to-front propagation, documented by the high and significant values of $\gamma^2_{21}(\alpha), \gamma^2_{31}(\alpha), \gamma^2_{41}(\alpha)$, and $\gamma^2_{42}(\alpha)$, together with the nonsignificant values of $\gamma^2_{12}(\alpha), \gamma^2_{13}(\alpha), \gamma^2_{14}(\alpha)$, and $\gamma^2_{24}(\alpha)$. A left-to-right propagation [significant $\gamma^2_{32}(\alpha)$ and nonsignificant $\gamma^2_{23}(\alpha)$] was also documented for this subject. The PDC [see Fig. 6(d)] evidenced that the propagation of the α rhythm occurs through the direct connections $y_1 \to y_2, y_1 \to y_3, y_2 \to y_3$, and $y_2 \to y_4$, while the causality relation $y_1 \Rightarrow y_4$ is not direct as $\pi^2_{41}(\alpha)$ is nonsignificant; note that $\pi^2_{21}(\alpha)$ is regarded as significant only using CFTd surrogates.

Results extended to the eight subjects are summarized in Table II. According to the coherence results averaged in the α-band, a significant coupling was observed between each pair of cortical regions. The high DC and PDC values in the

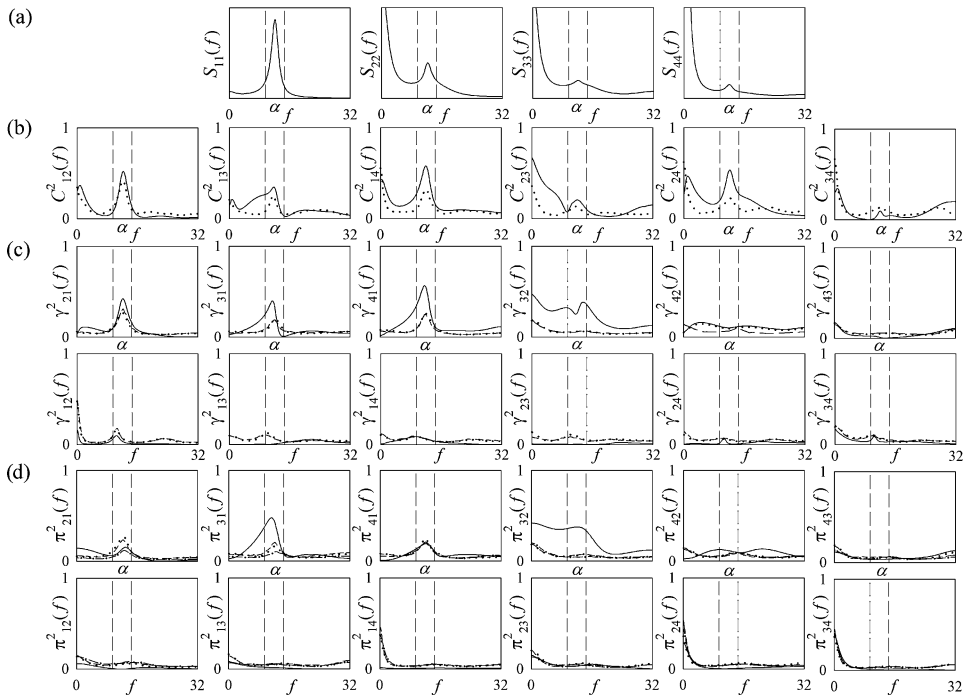

Fig. 6. Frequency-domain analysis of the occipital (y_1), left central (y_2), right central (y_3), and frontal (y_4) EEG time series in a representative subject. Plots and symbols are as in Fig. 5. Vertical lines mark the boundaries of the α-frequency band.

TABLE II
SUMMARY OF FREQUENCY-DOMAIN ANALYSIS FOR OCCIPITAL (y_1), LEFT CENTRAL (y_2), RIGHT CENTRAL (y_3), AND FRONTAL (y_4) EEG TIME SERIES

	C	n_{FT}	DC	n_{FT}	n_{CFTf}	PDC	n_{FT}	n_{CFTf}	n_{CFTd}
1→2	0.33	8	0.28	8	8	0.20	8	4	3
2→1			0.02	$0^{\S}$	$0^{\S}$	0.02	$0^{\S}$	$0^{\S}$	0
1→3	0.19	4	0.16	4	5	0.18	4	3	3
3→1			0.04	1	1	0.04	$0^{\S}$	0	0
1→4	0.34	8	0.29	8	8	0.14	2	2	2
4→1			0.03	$0^{\S}$	$0^{\S}$	0.02	1	1	1
2→3	0.36	8	0.30	8	8	0.32	8	8	8
3→2			0.04	$0^{\S}$	$0^{\S}$	0.03	$0^{\S}$	$0^{\S}$	$0^{\S}$
2→4	0.24	7	0.04	1	1	0.12	6	6	6
4→2			0.03	1	1	0.03	$1^{\S}$	$1^{\S}$	$1^{\S}$
3→4	0.13	5	0.11	5	5	0.15	5	5	5
4→3			0.04	$1^{\S}$	$1^{\S}$	0.05	$1^{\S}$	$1^{\S}$	$1^{\S}$

Symbols are as in Table I. Spectral functions are evaluated within the α-frequency band of EEG signals.

back-to-front directions compared to the opposite directions documented the presence of a propagation of the α activity from the posterior to the central and anterior cortical regions. This result is consistent with the notion that the α rhythm of the EEG originates in the occipital visual cortex, and then, spreads toward the central and frontal brain areas [26]. The result is strengthened by the surrogate data analysis, showing that the number of subjects with significant DC or PDC was statistically higher over the back-to-front than over the front-to-back directions (McNemar test). We note that utilization of CFTd surrogates led to statistical significance of this difference (not observed using FT surrogates) for the PDC from the occipital to the central cortical regions.

The PDC suggested that the information flow is not direct from the occipital visual cortex to the frontal cortical regions (π^2_{41} was significant only in two out of eight subjects), but is mediated by the left and right central areas, as documented by the significance of π^2_{21} and π^2_{42}, and of π^2_{31} and π^2_{43}, respectively. Another interesting observation is that the causal coupling originating in the posterior areas was stronger when directed toward the left central regions than toward the right central regions (γ^2_{21} and π^2_{21} were significant in more subjects than γ^2_{31} and π^2_{31}). Moreover, an evident direct unidirectional interaction occurred from the left to the right central areas, as documented by the PDCs π^2_{32} (always significant) and π^2_{23} (never significant). These observations agree with a previous study [27] showing that during eyes closed wakefulness the sources of EEG activity are mainly located in the left occipital areas, and propagation occurs from these areas toward right and anterior cortical sites.

VI. DISCUSSION

This study introduces a new hypothesis-testing framework for the frequency domain assessment of causality in MV time series. The framework integrates together the nonparametric (i.e., FT-based [28]) and parametric (i.e., based on bootstrap procedures [29]) approaches for MV surrogate data generation to impose the power spectrum of the original series and the phase relations according to the null hypothesis of absence of causality, respectively, along a predetermined direction of interaction. Although, the method can be seen as an extension of the nonparametric FT approach, the role played by the parametric part of the implementation is crucial, as it allows the overcoming of the limitations of phase randomization. Moreover, it gives flexibility to the overall implementation. Indeed, due to the

possibility to switch off either a part or the whole set of the model coefficients describing the causal interaction under analysis, the CFT method can be exploited to test for direct causality according to the original Granger' definitions [9], [10] using CFTd surrogates, or to test for an extended form of causality, including also indirect causal effects using CFTf surrogates. It is worth noting that in the generation of CFTf surrogates different solutions can be taken to nullify indirect causality from one series to another. In this study, we set to zero both the coefficients describing direct causal effects exiting from the input series and the coefficients describing direct causal effects entering the output series, even though only one of these zero setting procedures would have been sufficient to destroy the full causal coupling. This choice excluded to leave untouched connections without giving any plausible reason.

The reported simulation examples and applications to real-biological processes demonstrated that utilization of CFT surrogates improves the detection of frequency-domain causality in MV time series, depending on the specific concept of causality, which is under investigation. CFTf and CFTd surrogates, when associated with the DC and the PDC, respectively, were found to be best suited to detect causality and direct causality. On the contrary, FT surrogates, which are best suited to detect the noncausal coupling measured through the coherence [14], may be inappropriate to detect frequency-domain causality. In simulations, we reported instances of MVAR processes in which FT surrogates determined a statistically significant lower specificity in the detection of causality, and lower sensitivity in the detection of direct causality, compared to CFTf and CFTd surrogates, respectively. In real-data applications, our results suggest that CFT surrogates highlight directionality in cardiorespiratory interactions and enlighten the causal connectivity patterns in multichannel EEG analysis. Thus, the proposed framework may be regarded as an improvement of the FT approach [16] constituting the reference method for assessing the significance of spectral causality estimators on the basis of their empirical distribution in absence of coupling [5], [6], [8]. Besides the results here presented, the improvement is expected as the FT method generates surrogate data according to the null hypothesis h_1 of absent coupling, but h_1 cannot be considered, a correct null hypothesis to test causality and direct causality. In fact, the absence of causality only along a given direction does not necessarily imply the absence of any form of causality, for example, causality along the reverse pathway might be present.

As regards the detection of direct causality, a procedure that shares the parametric part of our implementation, i.e., the iteration of a reduced MVAR model with some coefficients forced to zero, has been very recently proposed to test the significance of the PDC [30]. Unlike the CFTd algorithm here introduced, the method in [30] is flawed by the inability to reproduce the second-order properties of the individual original time series. This limitation may bias the test for absence of spectral causality, as it is known that the individual second-order properties of the observed series may have a strong impact on the level for significance of causal and noncausal frequency-domain coupling measures [5], [14]. This aspect is particularly critical in the evaluation of the significance of the DC, as the individual power spectrum is present in the denominator of the DC formulation [see (3)].

As possible developments of this study, the CFT approach can be extended further to reflect more closely the marginal distribution of the observed time series (e.g., through amplitude-adjusted isospectral surrogates [15]) as well as the distribution of the MVAR inputs (e.g., by drawing the innovations from model residuals [29]). Moreover, it can be proposed in association with different discriminating statistics known to be helpful to detect causality in the frequency domain (e.g., those based on the Geweke's framework for causality estimation [18]). An interesting extension of our simulations would concern evaluating the power of the test for zero causality as a function of model structure and data length, as well as studying the bias possibly introduced varying the frequency and strength of oscillations occurring outside the considered frequency band.

APPENDIX

The MVAR model (2) was identified [20] first, estimating the coefficients of the corresponding strictly causal model (with no instantaneous effects: $\mathbf{B}(0) = 0$) through the standard least squares, then applying the Cholesky decomposition [3] on the covariance matrix of the residuals to estimate $\mathbf{B}(0)$ and the diagonal covariance matrix $\mathbf{\Sigma_W}$, and finally, using the estimated $\mathbf{B}(0)$ to calculate $\mathbf{B}(k)$ $(k = 1, \ldots, p)$. As a result of the Cholesky decomposition, a lower triangular structure is imposed for the matrix $\mathbf{B}(0)$. This constraint implies that the direction of the instantaneous effects is implicitly set by the ordering of the time series. In practical applications, this *a priori* restriction can be fulfilled on the basis of physical considerations in the case of beat-to-beat cardiovascular variability series, while the choice is less straightforward in the case of sampled versions of multiple continuous-time signals, such as the EEG [20].

The model order p was selected according to the multichannel version of the Akaike Information Criterion (AIC) [31]. Although this criterion is widely used, a comparison with approaches using the Bayesian framework [32] would be interesting. Model validation was performed checking whiteness and uncorrelation of the model residuals [31]. We remark that the fulfillment of MVAR identification hypotheses is required not only to guarantee that the frequency-domain coupling estimates capture the full second-order statistics of the original series, but also to let the surrogate series retain correctly the desired phase information.

REFERENCES

[1] E. Pereda, R. Q. Quiroga, and J. Bhattacharya, "Nonlinear multivariate analysis of neurophysiological signals," *Prog. Neurobiol.*, vol. 77, pp. 1–37, 2005.

[2] A. Porta, F. Aletti, F. Vallais, and G. Baselli, "Multimodal signal processing for the analysis of cardiovascular variability," *Phi. Trans. R. Soc A*, vol. 367, pp. 391–409, 2009.

[3] S. M. Kay, *Modern Spectral Estimation. Theory & application*. Englewood Cliffs, NJ: Prentice-Hall, 1988.

[4] L. A. Baccala, K. Sameshima, G. Ballester, A. C. Valle, and C. Timo-Iaria, "Studying the interaction between brain structures via directed coherence and Granger causality," *Appl. Signal Process.*, vol. 5, pp. 40–48, 1998.

[5] A. Porta, R. Furlan, O. Rimoldi, M. Pagani, A. Malliani, and P. van de Borne, "Quantifying the strength of the linear causal coupling in closed loop interacting cardiovascular variability signals," *Biol. Cybern.*, vol. 86, pp. 241–251, 2002.
[6] M. Kaminski, M. Ding, W. A. Truccolo, and S. L. Bressler, "Evaluating causal relations in neural systems: Granger causality, directed transfer function and statistical assessment of significance," *Biol. Cybern.*, vol. 85, pp. 145–157, 2001.
[7] L. A. Baccala and K. Sameshima, "Partial directed coherence: A new concept in neural structure determination," *Biol. Cybern.*, vol. 84, pp. 463–474, 2001.
[8] G. Nollo, L. Faes, A. Porta, R. Antolini, and F. Ravelli, "Exploring directionality in spontaneous heart period and systolic pressure variability interactions in humans. Implications in baroreflex gain evaluation," *Amer. J. Physiol.*, vol. 288, pp. H1777–H1785, 2005.
[9] C. W. J. Granger, "Investigating causal relations by econometric models and cross-spectral methods," *Econometrica*, vol. 37, pp. 424–438, 1969.
[10] C. W. J. Granger, "Testing for causality: A personal viewpoint," *J. Econom. Dyn. Control*, vol. 2, pp. 329–352, 1980.
[11] M. Eichler, "On the evaluation of information flow in multivariate systems by the directed transfer function," *Biol. Cybern.*, vol. 94, pp. 469–482, 2006.
[12] L. H. Koopmans, *The Spectral Analysis of Time Series*. New York: Academic, 1974.
[13] B. Schelter, M. Winterhalder, M. Eichler, M. Peifer, B. Hellwig, B. Guschlbauer, C. H. Lucking, R. Dahlhaus, and J. Timmer, "Testing for directed influences among neural signals using partial directed coherence," *J. Neurosci. Methods*, vol. 152, pp. 210–219, 2006.
[14] L. Faes, G. D. Pinna, A. Porta, R. Maestri, and G. Nollo, "Surrogate data analysis for assessing the significance of the coherence function," *IEEE Trans. Biomed. Eng.*, vol. 51, no. 7, pp. 1156–1166, Jul. 2004.
[15] T. Schreiber and A. Schmitz, "Surrogate time series," *Physica D*, vol. 142, pp. 346–382, 2000.
[16] J. Theiler, S. Eubank, A. Longtin, B. Galdrikian, and J. D. Farmer, "Testing for nonlinearity in time series: The method of surrogate data," *Physica D*, vol. 58, pp. 77–94, 1992.
[17] L. Faes, A. Porta, and G. Nollo, "Surrogate data approaches to assess the significance of directed coherence: Application to EEG activity propagation," in *Proc. 31st Conf. IEEE-EMBS*, 2009, pp. 6280–6283.
[18] Y. Chen, S. L. Bressler, and M. Ding, "Frequency decomposition of conditional Granger causality and application to multivariate neural field potential data," *J. Neurosci. Methods*, vol. 150, pp. 228–237, 2006.
[19] A. Hyvarinen, S. Shimizu, and P. O. Hoyer, "Causal modelling combining instantaneous and lagged effects: An identifiable model based on non-Gaussianity," in *Proc. Int. Conf. Mach. Learning (ICML2008)*, pp. 424–431.
[20] L. Faes and G. Nollo, "A method to assess frequency domain causality in the presence of instantaneous effects and its application to short term cardiovascular variability," *Meth. Inform. Med.*, 2010, to be published.
[21] L. Baccala, K. Sameshima, and D. Y. Takahashi, "Generalized partial directed coherence," in *Proc. 15th Int. Conf. Digital Signal Process.*, 2007, pp. 163–166.
[22] A. Malliani, *Principles of Cardiovascular Neural Regulation in Health and Disease*. Norwell, MA: Kluwer, 2000.
[23] J. A. Taylor and D. L. Eckberg, "Fundamental relations between short-term RR interval and arterial pressure oscillations in humans," *Circulation*, vol. 93, pp. 1527–1532, 1996.
[24] J. P. Saul, R. D. Berger, M. H. Chen, and R. J. Cohen, "Transfer function analysis of autonomic regulation. II. Respiratory sinus arrhythmia," *Amer. J. Physiol.*, vol. 256, pp. H153–H161, 1989.
[25] R. W. deBoer, J. M. Karemaker, and J. Strackee, "Hemodynamic fluctuations and baroreflex sensitivity in humans: A beat-to-beat model," *Amer. J. Physiol.*, vol. 253, pp. H680–H689, 1987.
[26] R. Kus, M. Kaminski, and K. J. Blinowska, "Determination of EEG activity propagation: Pair-wise versus multichannel estimate," *IEEE Trans. Biomed. Eng.*, vol. 51, no. 9, pp. 1501–1510, Sep. 2004.
[27] M. Kaminski, K. Blinowska, and W. Szclenberger, "Topographic analysis of coherence and propagation of EEG activity during sleep and wakefulness," *Electroencephalogr. Clin. Neurophysiol.*, vol. 102, pp. 216–227, 1997.
[28] J. Theiler and D. Prichard, "Constrained-realization Monte Carlo method for hypothesis testing," *Physica D*, vol. 94, pp. 221–235, 1996.
[29] D. N. Politis, "The impact of bootstrap methods on time series analysis," *Stat. Sci.*, vol. 18, pp. 219–230, 2003.
[30] J. R. Sato, D. Y. Takahashi, S. M. Arcuri, K. Sameshima, P. A. Morettin, and L. A. Baccala, "Frequency domain connectivity identification: An application of partial directed coherence in fMRI," *Hum. Brain Mapp.*, vol. 30, pp. 452–461, 2009.
[31] H. Lutkepohl, *Introduction to Multiple Time Series Analysis*. Berlin Heidelberg, Germany/New York: Springer-Verlag, 1993.
[32] W. Penny and S. Roberts, "Bayesian multivariate autoregressive models with structured priors," *IEEE Proc. Vision, Signal Image Processing*, vol. 149, no. 1, pp. 33–41, Feb. 2002.

Luca Faes (M'07) was born in Calceranica, Trento, Italy, in 1973. He received the M.S. degree in electronic engineering from the University of Padova, Padova, Italy, in 1998, and received the Ph.D. degree in electronic devices from the University of Trento, Trento, in 2003.

He was a Research Fellow of system identification and modeling at the Medical Biophysics Division, Institute for Scientific and Technologies Research, Trento, until 2000. He is currently engaged with the Department of Physics, Biosignals Laboratory, University of Trento. His research interests include time-series analysis, digital signal processing, and system modeling applied to mechanisms of cardiovascular control, atrial fibrillation, and brain activity.

Alberto Porta (M'09) was born in 1964. He received the M.S. degree in electronic engineering, in 1989, and received the Ph.D. degree in biomedical engineering from Politecnico di Milano, Milano, Italy, in 1998.

He was a Research Fellow of automatic control and system theory in the Department of Electronics for Automation, University of Brescia, Brescia, Italy, until 1994. Since 1999, he has been with the Faculty of Medicine, University of Milan, Milan, Italy, where he has been a Researcher, since 2005, teaching medical physics, since 2006, and applied medical statistics, since 2007. His current research interests include time-series analysis, biomedical signal processing, complexity analysis, and system identification and modeling applied to cardiovascular control mechanisms.

Giandomenico Nollo (M'07) was born in 1960. He received the M.S. degree in physics from the University of Trento, Trento, Italy, and the Ph.D. degree in physiology from the University of Torino, Torino, Italy.

He was a Research Fellow at the Division of Medical Biophysics, Institute for Scientific and Technologies Research, Trento, where, from 1989, he was a Researcher. Since 2000, he has been with the Department of Physics, University of Trento, where he is teaching biomedical instrumentation and monitoring of biosystems for the *Laurea* in physics in the Faculty of Science. His current research interests include monitoring of human biosignals, and linear and nonlinear modeling of physiological data.